
RESEARCH PAPER

# *Spectral Dependence of Photovoltaic Cell Conversion Efficiency for Monochromatic Radiation*

Terubumi Saito* and Minato Takesawa

Department of Environmental Information Engineering, Graduate School, Tohoku Institute of Technology, 35-1 Yagiyamakasumi-cho, Taihaku-ku, Sendai, Miyagii, Japan
*Corresponding author. E-mail: tsaito-pv@tohtech.ac.jp

## *Abstract*

Theoretical limit of solar cell conversion efficiency given by Shockley and Queisser is calculated for the case that the cell is illuminated by solar radiation. If the input radiation is monochromatic, the efficiency can exceed the limit. The aim of our study is to experimentally demonstrate this theoretical prediction and to obtain the experimental results of spectral dependence of photovoltaic cell conversion efficiency. Conversion efficiencies of two types of Si photodiodes (equivalent to solar cells) are determined through the measurements of current–voltage characteristics as a function of the wavelength and the incident radiant power. As the theory predicts, it has been confirmed that the conversion efficiency is almost proportional to the wavelength and also to the logarithm of the incident radiant power. Also, it has been experimentally confirmed that the power conversion efficiency for long wavelength monochromatic radiation is higher than that for white radiation.

*Keywords:* photovoltaic cell, conversion efficiency, spectral dependence, monochromatic radiation, Shockley–Queisser limit, photodiode, fill factor, current–voltage characteristics

*Citation*
Terubumi Saito and Minato Takesawa (2022), Spectral Dependence of Photovoltaic Cell Conversion Efficiency for Monochromatic Radiation. *Green Energy and Environmental Technology* 2022(0), 1–19.

*DOI*
https://doi.org/10.5772/geet.02



*Published*
28 March 2022

## *1. Introduction*

A photovoltaic cell (also called a solar cell) is a semiconductor device that partially converts radiant power into electrical power. the most widespread type of solar cell is crystalline Si-based solar cells. Currently, the highest conversion efficiency of single junction monocrystalline Si solar cell module is reported to be 26.1% [1]. Even with triple-junction compound type mainly targeted for space use, top efficiency is still 39.5% [1]. The theoretical marginal efficiency known as the Shockley–Queisser limit is 32.7% for single junction solar cells [2] and 29.4% for crystalline Si solar cells [3]. The limit is calculated for the case that the cell is illuminated by solar radiation.

Factors to decrease the conversion efficiency [4, 5] are categorized into the following: (1) Optical losses [6] such as reflection at the surface and transmission

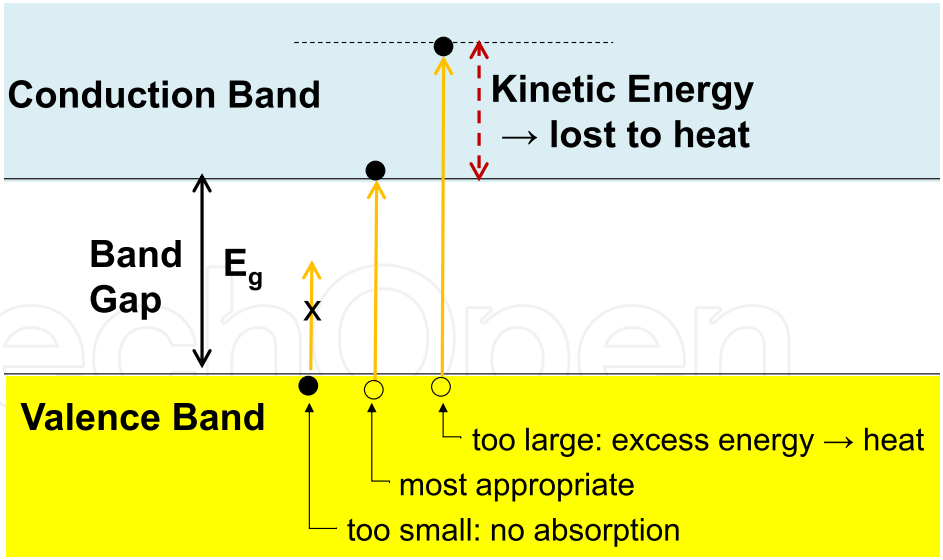


*Figure 1.* Energy band diagram showing the relationship between the bandgap energy and the incident photon energy for photovoltaic cells.

through the substrate, (2) Carrier recombination losses [7] at the surfaces of and in the substrate, (3) Joule heating in the series and shunt resistance, (4) Mismatch in resistance between the source and the load, and (5) Mismatch in energy between the semiconductor bandgap and the incident photon energy. Continuous efforts made it possible to steadily decrease the losses of the first four types and approach its limit of nearly zero.

However, concerning the loss (5), it is, in principle, difficult to decrease due to the fact that the sun, the source of the incident radiation, has a very wide spectrum. Figure 1 shows a schematic energy band diagram of photovoltaice cells. If the photon energy is below the bandgap energy of the material, the material is transparent and therefore the energy cannot be utilized at all. On the other hand, if the photon energy is greater than the bandgap, the excess energy of photo-excited electrons between the excited level and the bottom of the conduction band is finally lost to the heat, and thus the conversion efficiency becomes low. Based on the above consideration, it is theoretically expected that the conversion efficiency of solar cells will increase and even can exceed the Shockley–Queisser limit if monochromatic radiation with photon energy near the band gap is injected.

From the application side, the need for wireless power transmission [8, 9] has been increasing, for instance, for power beaming to flying drones, spacecrafts [9, 10] etc. For such a distant power beaming, stronger interest has emerged in the optical system [11, 12] consisting of laser diodes (or light emitting diodes) and photovoltaic cells, rather than the traditional electromagnetic induction system. For the optical

power transmission purposes using a laser beam, conversion efficiency measurement results over the Shockley–Queisser limit have been already reported [13] for specially designed cells at a discrete wavelength. However, there are no systematic investigations for commercially available conventional solar cells in a wide spectral range.

The purpose of this study is to measure the power conversion efficiency of solar cells for various wavelengths of radiation and to experimentally verify the wavelength dependence of the power conversion efficiency, with the intention of providing the basis for future applications of more efficient ways to use the solar cells.

## 2. Theoretical

### 2.1. $I$–$V$ characteristics of photovoltaic cell

Current–voltage characteristics of an ideal photovoltaic cell is given by

$$I = I_L - I_0 \left[ \exp\left( \frac{eV}{nkT} \right) - 1 \right] \tag{1}$$

where $I$ is the current that flows in an external circuit, $I_L$ the light-generated current, $V$ the forward voltage across the diode, $I_o$ saturation current, $n$ the ideality factor, $k$ Boltzmann constant, and $T$ the junction temperature.

Curve A in figure 2 is such a $I$–$V$ characteristic under a certain irradiated condition. The intersection point with the vertical axis is termed short circuit current, $I_{sc}$, which is given by setting $V = 0$ and it holds that

$$I_{sc} = I_L. \tag{2}$$

The intersection point with the horizontal axis is termed open circuit voltage, $V_{oc}$, which is given by setting $I = 0$ and becomes

$$V_{oc} = \frac{nkT}{q} \ln\left( \frac{I_L}{I_0} + 1 \right). \tag{3}$$

If the incident optical power is large enough to satisfy $I_L \gg I_o$, equation (3) shows that $V_{oc}$ is nearly proportional to the logarithm of $I_L$. When the radiant power incident on the photodiode is increased, the curve moves outward as shown by curve B. When one sees short-circuit current, the current output is increased as a linear function of the radiant power (operating point moves along the vertical axis). On the other hand, if one sees open-circuit voltage, the voltage output is increased as a logarithmic function of the radiant power if $I_L \gg I_o$, as expressed by

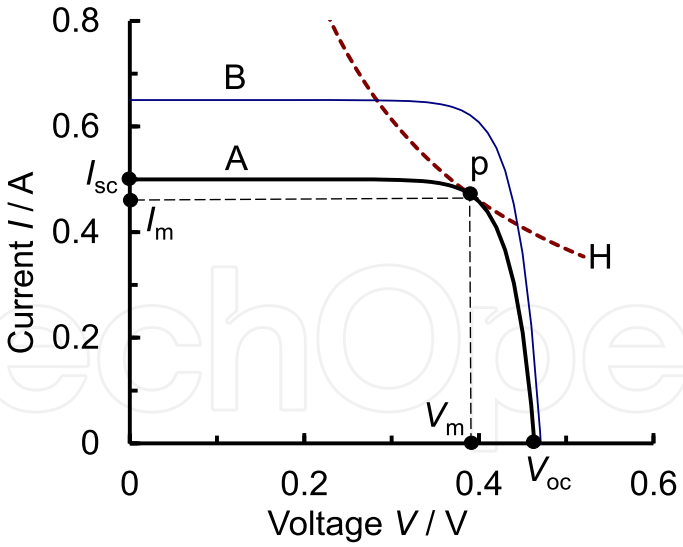


*Figure 2.* Current–voltage characteristics of a virtual photodiode to illustrate its measuring conditions. See text for details.

equation (3) (operating point moves along the horizontal axis). Actual operating condition always lies between these two extremes. If the load resistance is small enough compared to the cell shunt resistance to satisfy the constant current condition, the current measured is almost equal to the short circuit current and is proportional to the incident radiation flux. For the purpose of power generation like in solar cells, it is important to match the appropriate load resistance to obtain the maximum power, whose operating point is shown by point, $p$, which is a tangent point to a hyperbolic curve, a locus to give a constant power.

## 2.2. Effects of series-/shunt-resistance etc.

Actual photovoltaic cells are not as simple as modeled in equation (1) since they generally have a series resistance, $R_s$, and a shunt resistance, $R_{sh}$, inside them. Ideally, the series resistance should be 0 and the shunt resistance should be ∞. Both resistors affect the current–voltage characteristics and reduce the *FF*. A high series resistance decreases the short circuit current, and its value is roughly approximated by the absolute value of the inverse of the slope in *I*–*V* plane (horizontal axis: *V*) near the open circuit voltage point. On the other hand, a low shunt resistance decreases the open circuit voltage, and its value is roughly approximated by the absolute value of the inverse of the slope near the short circuit current point. Characteristic equation for actual photovoltaic cells with the effects of these resistances is given by the following equation [14].

$$I = I_L - I_0 \left\{ \exp\left[ \frac{e(V + IR_s)}{nkT} \right] - 1 \right\} - \frac{V + IR_s}{R_{Sh}}. \quad (4)$$

By curve fitting, $R_s$, $R_{sh}$ and $n$ were obtained. Fill factors and conversion efficiencies etc. can be corrected by using these parameters.

## 2.3. Solar cell power conversion efficiency

In general, photovoltaic cell conversion efficiency, $\varepsilon$, is given by the following equation,

$$\begin{aligned} \varepsilon &= P_e/P_r \\ &= FFV_{oc}I_{sc}/P_r, \end{aligned} \tag{5}$$

where $P_e$ is the output electrical power, $P_r$ the incident (input) radiant power, $FF$ the fill factor, $V_{oc}$ the open circuit voltage, and $I_{sc}$ the short circuit current. The fill factor is obtained by measuring the current–voltage characteristics through the following equation,

$$FF = \frac{V_m I_m}{V_{oc} I_{sc}} = \frac{P_m}{V_{oc} I_{sc}}, \tag{6}$$

where $V_m$ and $I_m$ are the voltage and the current that give the maximum power output, respectively. The fill factor can be obtained by measuring the current–voltage characteristics, which are typically 0.7 to 0.85 for commercially available solar cells. As stated before, the fill factor is affected by existence of series resistance and shunt resistance.

For determination of the conversion efficiency, it is easy to measure $FF$, $V_{oc}$ and $I_{sc}$ in equation (5). In contrast, $P_r$ determination is not simple for solar spectrum and tends to bring large uncertainty because it needs spectral integration. Also, it should be stressed that conversion efficiency depends on the spectral distribution of the input radiation even if $P_r$ is kept constant. Therefore, IEC60904-3 standard [15] defines the use of solar radiation with spectrum of AM1.5G at the irradiance of 1 kW/m² as input radiation for measurements of solar cell conversion efficiency. In this study, we extend the definition by replacing the solar radiation with (quasi-)monochromatic radiation at an arbitrary irradiance level.

Equation (5) shows that if $FF$ can be assumed to be a constant, the conversion efficiency is proportional to the open-circuit voltage that is almost proportional to the logarithm of the incident radiation flux. In reality, $FF$ increases slightly as the incident radiant flux increases. The following are empirical equations to give $FF$ as a

function of $V_{oc}$ [16 , 17].

$$FF = FF_0\left\{1 - \frac{FF_0(v_{oc}+0.7)}{v_{oc}\, r_{sh}}\right\} \quad (7)$$

$$v_{oc} = \frac{V_{oc}}{nkT/q} \quad (8)$$

$$r_{sh} = \frac{R_{sh}}{R_{ch}} \quad (9)$$

$$R_{ch} = \frac{V_{oc}}{I_{sc}}. \quad (10)$$

Notations are as follows. $FF_o$: ideal fill factor without considering internal resistance, $v_{oc}$: normalized voltage, $r_{sh}$: normalized shunt resistance, $R_{sh}$: shunt resistance in $\Omega$, $R_{ch}$: characteristic resistance of solar cell.

## 2.4. Solar cell conversion efficiency for monochromatic radiation

In the case that the incident radiation is monochromatic with the photon energy $E_p$ and photon flux $\Phi$, the incident radiant flux is given by $P_r = \Phi E_p$. If the spectral external quantum efficiency for $E_p$ is $\eta$, then it holds that $I_{sc} = e\Phi\eta$ where $e$ is the elementary electronic charge. Therefore,

$$\begin{aligned}\varepsilon &= \frac{P_e}{P_r} \\ &= \frac{FFV_{oc}I_{sc}}{\Phi E_p} \\ &= \frac{e\eta FFV_{oc}}{E_p}.\end{aligned} \quad (11)$$

If the photon energy, $E_p$, is expressed in eV and the open circuit voltage, $V_{oc}$, is expressed in $V$, then

$$\varepsilon = \frac{\eta FFV_{oc}}{E_p} = \frac{\eta FFV_{oc}\lambda}{1240}. \quad (12)$$

It shows that the conversion efficiency is expected to be inversely proportional to the photon energy or it is expected to be proportional to the wavelength, provided that $\eta FFV_{oc}$ is constant. Rigorously speaking, equation (7) shows that $FF$ slightly increases as $V_{oc}$, or logarithm of $I_L$ increases, and equation (3) shows that $V_{oc}$ is nearly proportional to the logarithm of $I_L$.

In addition, the incident radiant flux can be expressed in terms of the spectral responsivity $s$ [A/W] as follows

$$P_{in} = \frac{I_{sc}}{s}. \quad (13)$$

Therefore, the power conversion efficiency $\varepsilon$ is

$$\varepsilon = FFV_{oc}s. \tag{14}$$

As explained, *FF* slightly increases as $I_L$, or incident optical power, increases and $V_{oc}$ is nearly proportional to the logarithm of $I_L$. Therefore, the power conversion efficiency $\varepsilon$ increases slowly as the incident optical power increases. If it can be approximated that *FF* and open-circuit voltage are constants, the power conversion efficiency is also proportional to the spectral responsivity.

# 3. Experiments

## 3.1. Measurement targets

Solar cell products commercially available are products contained in a module with large area composed of many cells connected in series. This renders it difficult to perform our spectral cell characterization in detail because it requires large uniform monochromatic radiation sources and moreover, individual cell characterization is almost impossible without adding electrical wiring between the cells. Therefore, we chose to use silicon photodiodes instead of solar cells.

We have investigated on two types of Si photodiodes (S1227-1010BQ [18] and S1337-1010BQ [19]) made by Hamamatsu Photonics, both of which are designed as a photodetector but also work as a solar cell based on the same principle of operation. Both photodiodes have photosensitive area of 1 $cm^2$ and are known to have an internal quantum efficiency of almost unity meaning that there are no recombination losses [20, 21]. Major difference is that S1227-1010BQ has a thinner depletion region of pn junction while S1337-1010BQ has a thicker depletion region of pn junction.

Measured external spectral quantum efficiencies of the photodiodes are shown in figure 3. The external spectral quantum efficiency is defined as the number of electron–hole pairs generated per unit time divided by the photon flux (number of photons per unit time) incident on the photodetector as a function of the wavelength. Note that S1337-1010BQ photodiode has nearly constant quantum efficiency covering a wider spectral range owing to the thicker depletion region. For the monochromatic radiation with photon energy, $E_p$ in J, spectral quantum efficiency, $\eta$, can be related to spectral responsivity, $s$ in A/W, as $s = e\eta/E_p$ where $e$ is an electronic charge. The spectral responsivity is used, based on equation (13), to determine the incident radiant flux required to obtain the conversion efficiency.

The wavelength at maximum spectral responsivity is 740 nm for S1227-1010BQ and 960 nm for S1337-1010BQ, respectively. Other differences in the series- and shunt-resistances revealed will be discussed later.

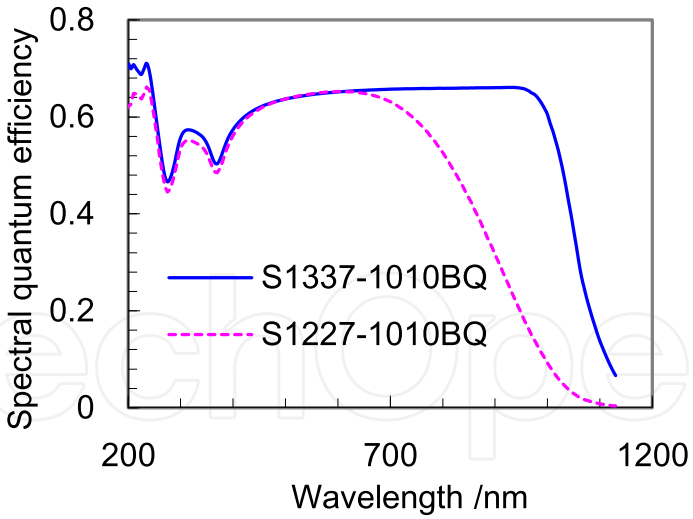


*Figure 3.* Spectral quantum efficiencies of the two types of photodiodes, S1337-1010BQ and S1227-1010BQ.

### 3.2. Radiation sources used

To characterize photovoltaic cells, various kinds of quasi-monochromatic radiation sources have been used as shown in table 1. The first category is a combination of a halogen incandescent lamp and one of the five interference filters, whose passband wavelengths are different. The output radiant power is relatively low, especially for the shorter wavelengths reflecting the spectral property of the halogen lamp. For realizing higher irradiance, as a second category, two types of laser diodes abbreviated as LDs (Hamamatsu Photonics L9418-72 and L10452-72) were used. As a third category, three colors of light emitting diodes abbreviated as LEDs (red: SANDER AH30-100TR, blue: SANDER AH30-100B, and green: Linkman HPL-H77FG1BA) were used.

Spectral irradiance measurements were conducted for all the sources using a NIST traceable array type spectrometer (Stellar Net Inc., BLUE-Wave) combined with a transmission diffuser (Stellar Net Inc., F600-UVVis-SR) as a photoreceptor and an optical fiber.

### 3.3. Measurements

In addition to the spectral irradiance measurements for various radiation sources and the spectral responsivity measurements for photodiodes, many efforts were paid to the current–voltage ($I$–$V$ ) characteristics measurements. This is necessary to determine $I_{sc}$, $V_{oc}$, $FF$, and finally the conversion efficiency of solar cells. The $I$–$V$ characteristics measurements are conducted mostly by using a DC source measure unit (SMU), ADCMT 6241A. A solar cell (photodiode) connected to the SMU is set

*Table 1.* Radiation sources used for cell characterization.

| Radiation source | Center* wavelength (nm) | FWHM (nm) | Peak spectral irradiance** (mW $m^{-2}$ $nm^{-1}$) |
|---|---|---|---|
| Incandesecnt lamp + interference filter | 864.5 | 29.0 | 140 |
| Incandesecnt lamp + interference filter | 795.0 | 19.5 | 117 |
| Incandesecnt lamp + interference filter | 697.8 | 19.5 | 60 |
| Incandesecnt lamp + interference filter | 622.0 | 28.0 | 46 |
| Incandesecnt lamp + interference filter | 490.3 | 21.5 | 8.2 |
| LD (L9418-72) | 979.5 | 14.0 | 754 |
| LD (10452-72) | 803.8 | 23.5 | 829 |
| Red LED (AH30-100TR) | 633.5 | 15.0 | 745 |
| Green LED (HPL-H77FG1BA) | 524.5 | 33.0 | 860 |
| Blue LED (AH30-100B) | 475.0 | 24.0 | 328 |

* Centroid wavelength or weighted mean (not peak wavelength) ** Typical values at a distance of 10 cm from the source.

in a dark room and is irradiated by a radiation source. An application program on the computer automatically scans the resistance of the SMU and measures the current flowing and voltage across the cell simultaneously to obtain *I–V* characteristics.

## 4. Results and Analysis

### 4.1. Current–voltage characteristics measurements at different wavelengths

As discussed in introduction, the difference between the incident photon energy and the bandgap energy is finally thermalized. This can be theoretically interpreted that the electrical output properties such as current–voltage characteristics do not depend on the incident photon energy.

To experimentally confirm this prediction, the current–voltage characteristics have been measured at different wavelengths for the same level of short-circuit

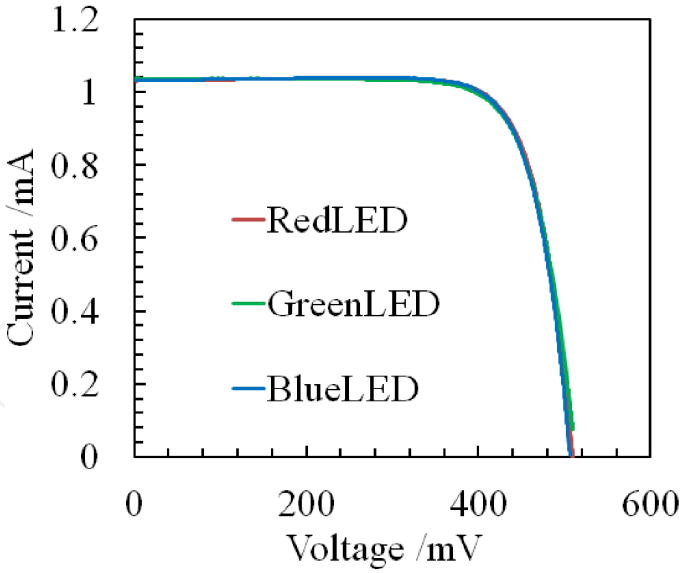


*Figure 4.* Wavelength dependence of S1227-1010BQ current–voltage characteristics at short-circuit current of 1 mA.

current. Figure 4 shows the results for red (616 nm), green (525 nm) and blue (475 nm) LEDs under the short-circuit current of 1 mA. Since each short-circuit current differs slightly, curves were translated in the Y-axis direction to match the short-circuit current. It was confirmed experimentally that the current–voltage characteristics and therefore, also the fill factor do not depend on the wavelength of the input radiation.

## 4.2. Current–voltage characteristics of Si photodiodes for various radiation sources at different irradiances

Current–voltage characteristics of both Si photodiodes S1337-1010BQ and S1227-1010BQ have been measured irradiated by various radiation sources under various levels of irradiances. One of the comparison measurements are shown in figure 5.

By curve fitting of equation (4) to the measured curves, it turns out that the difference in the *I–V* curves is attributed especially to the smaller shunt resistance for S1337-1010BQ. The parameters obtained by the curve fitting for S1337-1010BQ are $R_{sh}$ = 169 Ω, $R_s$ = 3. 41 Ω, $n$ = 4. 54, $I_o$ = 22. 8 μA and $I_L$ = 5. 70 mA under $T$ = 298.9 K and those for S1227-1010BQ are $R_{sh}$ = 104 kΩ, $R_s$ = 5. 42 Ω, $n$ = 1.38, $I_o$ = 1.01 nA and $I_L$ = 5. 45 mA under $T$ = 299.3 K. It should be noted that these values obtained are not unique but depend on each other. It is also noted that the values vary depending on the radiant intensity. Nevertheless, it is clear that S1337-1010BQ photodiodes have much smaller shunt resistance, in the high irradiance level, than S1227-1010BQ and

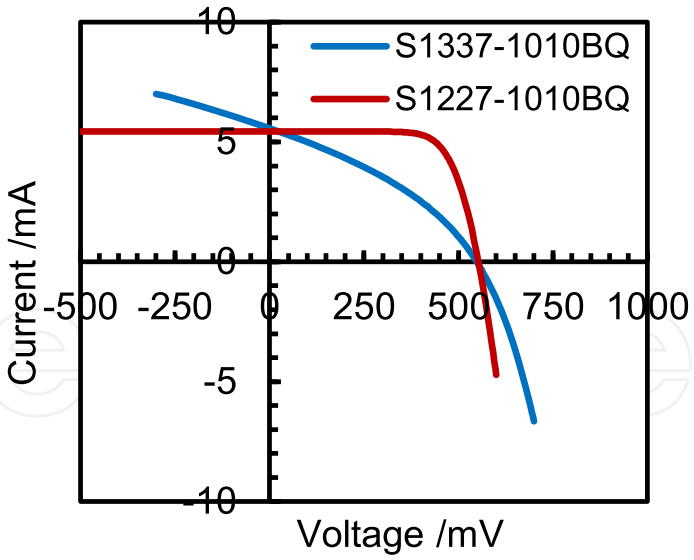


*Figure 5.* Current–voltage characteristics comparison under same short circuit current illuminated by green LED between S1337-1010BQ and S1227-1010BQ.

also than the nominal minimum value of 50 MΩ (at 10 mV) in the specification sheet. Therefore, the *I–V* curves for S1337-1010BQ are largely deformed at high irradiance level leading to the difficulty in deriving parameters such as conversion efficiency.

Current–voltage characteristics for S1227-1010BQ photodiode has been measured for various quasi-monochromatic sources as shown in figure 6. It is prominent that only the curve shape for 980 nm LD is largely different from other curves. At this wavelength, the spectral quantum efficiency of S1227-1010BQ photodiode is very low as shown in figure 3. It means the absorption is very weak and therefore, most of the incident photons passes through the silicon substrate and some photons may be reflected at the back surface. It is speculated that such special condition may decrease the shunt resistance.

Ideally, *I–V* characteristic curves should have the same shape. In other words, all the curves should overlap each other by shifting vertically. However, not only the 980 nm curve but also sunlight- and 525 nm-curves have shorter constant current straight line length than others. It can be interpreted that the voltage drop across the series resistance becomes visible in the higher current level.

As for the linearity of the short circuit current to the incident radiant power, S1337-1010BQ starts to exhibit nonlinearity above around 0.1 mA, while S1227-1010BQ is confirmed to be linear in the short circuit current range up to 5 mA except for 980 nm LD.

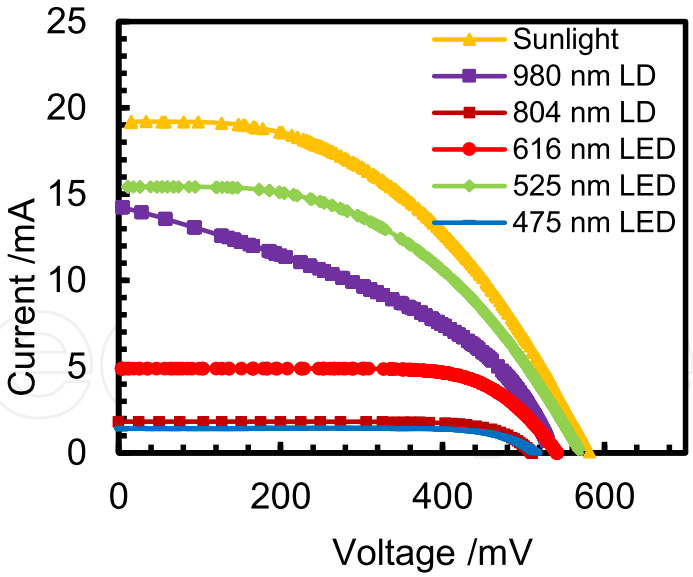


*Figure 6.* Current–voltage characteristics of Si photodiode (S1227-1010BQ) for various radiation sources.

### 4.3. Fill factors as a function of short circuit current

Figure 7 and figure 8 show fill factors as a function of short circuit current for S1337-1010BQ and S1227-1010BQ, respectively obtained from the current–voltage characteristics measurements. The data indicated by the arrows are after correcting for the shunt and series resistances.

Theoretically, the Fill Factor, *FF*, increases slightly as the incident radiation flux increases according to equation (7), but the results for S1337-1010BQ in figure 7 show that the *FF* tends to decrease as the short-circuit current, or incident radiation flux, increases for all radiation sources. Specifically, the maximum *FF* of 0.75 at the minimum short-circuit current of 0.002 mA (490 nm interference filter) falls to 0.35 at the maximum short-circuit current of 6.7 mA (804 nm laser diode). As discussed in Section 4.1, this seems to be caused mainly by the small shunt resistance of the S1337-1010BQ Si photodiode.

As for the results of S1227-1010BQ in figure 8, the *FF* is nearly constant up to a short-circuit current of about 2 mA, but it tends to decrease as the short-circuit current increases. This is because the series resistance of the Si photodiode affects the current–voltage characteristics as shown in figure 6, and this effect becomes more pronounced when the short-circuit current, which is proportional to the incident radiation flux, increases.

As shown in figure 8, measurement uncertainties for *FF* were not small enough to observe clear increasing trend to the radiant power. By substituting measured

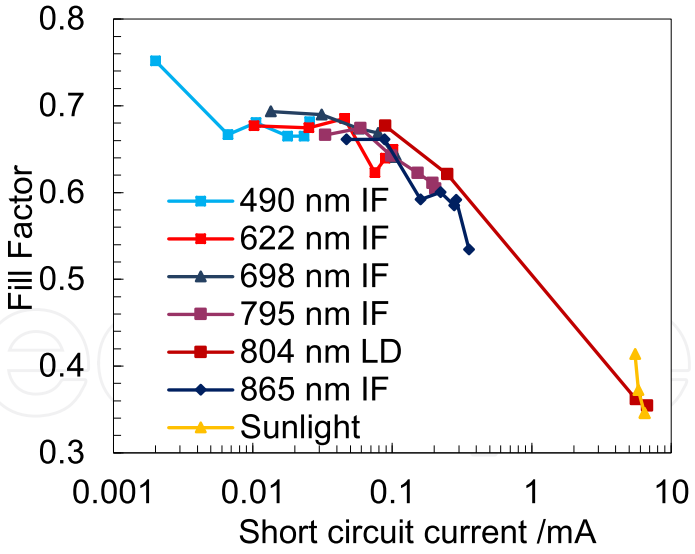


*Figure 7.* Fill factors of Si photodiode (S1337-1010BQ) as a function of short circuit current for different wavelength sources.

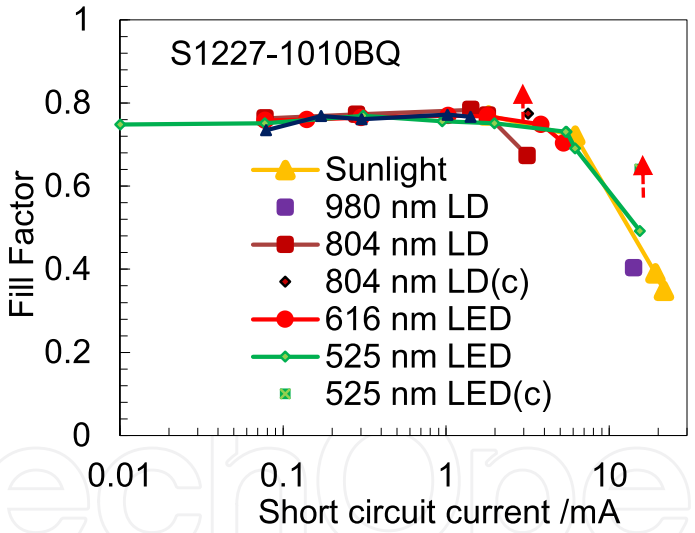


*Figure 8.* Fill factors of Si photodiode (S1227-1010BQ) for each radiation source.

parameters to equation (7)–(10), it turns out that *FF* is almost constant in the range surveyed in the measurements.

As for comparison between the two types of photodiodes, the results show that S1227-1010BQ can be used up to higher irradiance level by about one order of magnitude than S1337-1010BQ before the resistance effects appear. Both results confirm that *FF* does not depend on the wavelength of the incident radiation as also shown in Section 4.1.

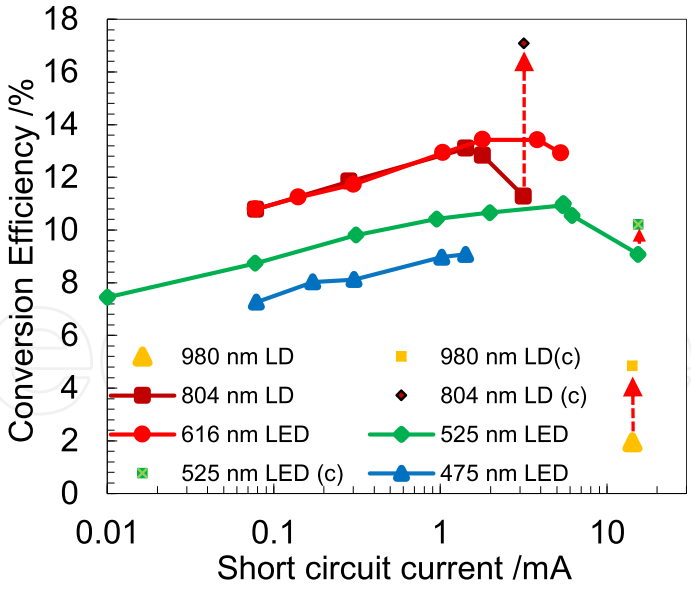


*Figure 9.* Conversion efficiency of Si photodiode (S1227-1010BQ) as a function of short circuit current for various monochromatic radiation sources.

## 4.4. Conversion efficiency as a function of short circuit current

Figure 9 shows conversion efficiencies as a function of short circuit current for S1227-1010BQ photodiode irradiated by various kind of quasi-monochromatic radiation derived based on equation (5) through the measurements of the current–voltage characteristics. The data indicated by the arrows are after correcting for the shunt and series resistances.

As expected, there exists a general increasing trend to the short circuit current or the radiant power across the sources except for higher short circuit current than 2 mA. The cause of the decrease in the high current is highly likely due to the decrease in *FF* as observed in figure 8 since the decrease in *FF* starts at the same currents. As discussed in Section 4.3, the cause of the decrease in *FF* is considered to be due to the non-negligible value of series resistance since the voltage drop by the series resistance becomes large as the current increases.

In figure 9, the conversion efficiency is plotted as a function of logarithm of short circuit current. The straight trend means that the conversion efficiency is proportional to the logarithm of the short circuit current or the logarithm of the radiant power. This result is supported by theory (equation (5)) under the condition that *FF* is constant since $V_{oc}$ in equation (5) is nearly proportional to the logarithm of the short circuit current according to equation (3).

In addition to the results shown in figure 9, conversion efficiency measurements for sunlight has been performed to compare efficiencies between monochromatic

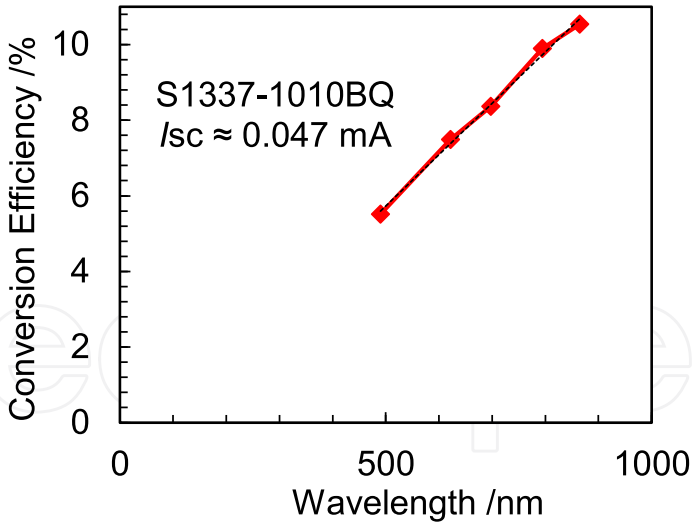


*Figure 10.* Wavelength dependence of conversion efficiency of Si photodiode (S1337-1010BQ) under the same short-circuit current of about 0.047 mA.

and white radiation. Under the same short circuit current of 1.8 mA, the measured conversion efficiencies of the Si photodiode (S1227-1010BQ) are 7.5% for sunlight, 15.8% for 804 nm LD, and 13.4% for red LED. Therefore, it is confirmed that the conversion efficiency for monochromatic radiation is higher than that of sunlight at the same level of short-circuit current.

## 4.5. Conversion efficiency as a function of wavelength

After numerous measurements for *I–V* characteristics on both types of photodiodes, it turns out that S1337-1010BQ has poorer performance under the high irradiance level due to the low shunt resistance as explained. Therefore, only a single conversion efficiency curve for S1337-1010BQ under the short-circuit current of about 0.047 mA, which corresponds to low irradiance, is shown in figure 10 as a function of wavelength. The sources used are Blue LED for 475 nm, Red LED for 631 nm and LD for 804 nm.

It shows that the conversion efficiency is proportional to the wavelength as predicted. This means that $\eta FFV_{oc}$ is constant to the wavelength. The result in figure 4 supports that it is true for *FF* and $V_{oc}$ since there are no spectral dependence under the same $I_{sc}$. As for $\eta$, refer to figure 3. The difference in quantum efficiencies of S1337-1010BQ in the wavelength range between 475 nm and 804 nm is only 4%. Therefore, the result is consistent.

Figure 11 shows similar results for S1227-1010BQ, which are differently presented as a function of wavelength but are based on the same results in figure 9. Note that

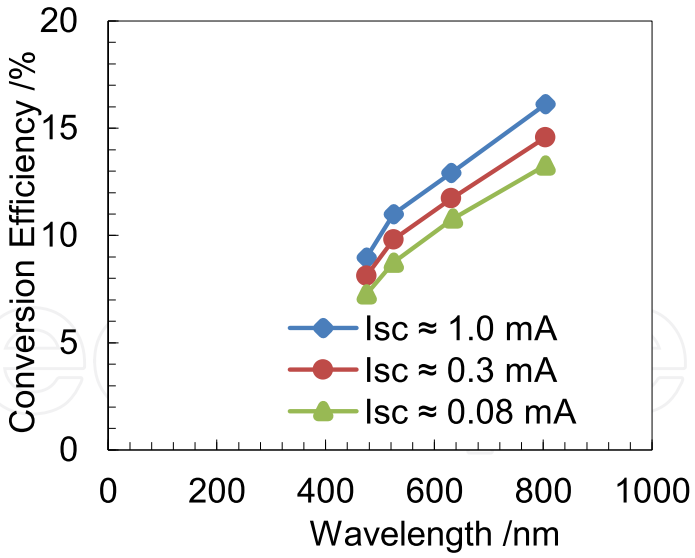


*Figure 11.* Wavelength dependence of (external) conversion efficiency of Si photodiode (S1227-1010BQ) under the three levels of short-circuit current.

the results cover much higher irradiance level than that for S1337-1010BQ thanks to the higher shunt resistance.

Again, an almost linear but a little distorted trend is obtained. The cause of the diversion from the straight line is considered to be due to the nonconstant spectral quantum efficiency of S1227-10101BQ as shown in figure (3). Contrary to recent solar cells, these photodiodes have no active anti-reflection measures and, therefore, have high reflectance of about 30%. Moreover, since S1227-1010BQ has a thinner depletion region, some portion of photons can pass through the substrate at long wavelength due to the weak absorption.

It is possible to correct for this effect by converting the measured (external) conversion efficiency, $\varepsilon_{ext}$, to internal conversion efficiency, $\varepsilon_{int}$. by the relationship,

$$\varepsilon_{int} = \frac{\eta_{int}}{\eta_{ext}} \varepsilon_{ext}, \tag{15}$$

where $\eta_{int}$ and $\eta_{ext}$ are internal and external quantum efficiency, respectively. As stated, $\eta_{int}$ is assumed to be unity. The internal conversion efficiency is defined by the electrical power generated divided by the radiant power *absorbed by* the detector. The external one differs in that the denominator is the radiant power *incident on* the detector. Similarly, the internal quantum efficiency is defined by the number of electron–hole pairs generated divided by the number of photons *absorbed by* the detector. The external one differs in that the denominator is the number of photons *incident on* the detector.

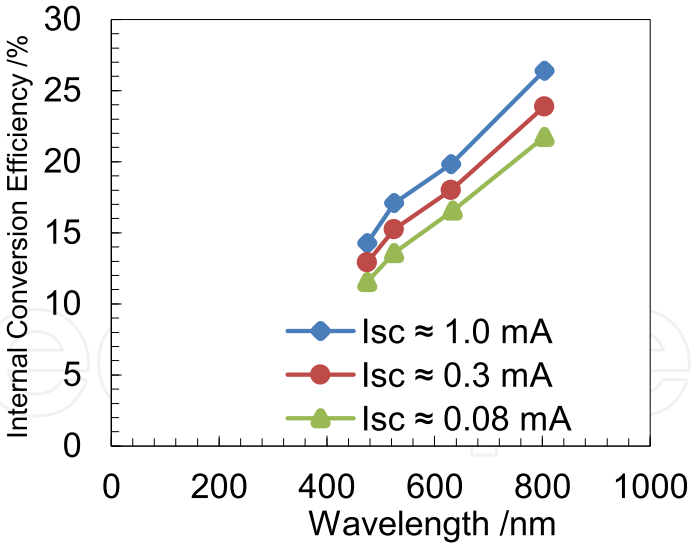


*Figure 12.* Wavelength dependence of internal conversion efficiency of Si photodiode (S1227-1010BQ) under the three levels of short-circuit current.

Graph converted to internal conversion efficiency is shown in figure 12. Better linearity to the wavelength is obtained. The efficiency in this graph means the conversion efficiency achievable if there is no reflection and transmission losses. The highest value is 26.4% at 804 nm for the short circuit current of 1.0 mA.

## 5. Conclusion

In this study, two types of Si photodiodes known to have almost unity internal quantum efficiency, different mainly in the depletion region thickness (S1337-1010BQ has a thicker one than S1227-1010BQ), are used for evaluation as photovoltaic cells. Their current–voltage characteristics have been measured at several wavelengths and at several irradiance levels to obtain fill factors and conversion efficiencies as a function of the wavelength and of the short circuit currents.

Through the comparison measurements, it turns out that S1337-1010BQ has smaller shunt resistance than S1227-1010BQ causing the decrease in fill factor and hence the conversion efficiency in the high irradiance level.

As theory predicts, it is confirmed that the short-circuit current is proportional to the incident radiant flux, the open-circuit voltage is nearly proportional to the logarithm of the incident radiant flux, and there is no wavelength dependence in the current–voltage characteristics at the same radiation intensity.

The measured conversion efficiency has been experimentally confirmed to be almost proportional to the wavelength of the incident radiation. It was also

confirmed that the conversion efficiency can be improved by injecting monochromatic radiation of long wavelength close to the band gap with high radiant flux, as predicted by the theory.

## *Data availability*

The data that support the findings of this study are available from the corresponding author, T.S., upon reasonable request.

## *Conflict of interest*

The authors declare no conflicts of interest associated with this article.

## *Acknowledgements*

The authors would like to thank Professor Iinuma for his kind guidance to this theme and his continuous support. This study was funded by the education/research funds of Tohoku Institute of Technology.

## *References*

1 **Best Research-Cell Efficiency Chart [Internet]**. Best Research-Cell Efficiency Chart. 2022 [cited 2022 Mar 2]. Available from: https://www.nrel.gov/pv/cell-efficiency.html.

2 **Shockley W., Queisser H. J.** Detailed balance limit of efficiency of *p–n* junction solar cells. ***J. Appl. Phys.***, 1961; **32**(3): 510–519.

3 **Richter A., Hermle M., Glunz S. W.** Reassessment of the limiting efficiency for crystalline silicon solar cells. ***IEEE J. Photovolt.***, 2013; **3**(4): 1184–1191.

4 **Wolf M.** Limitations and possibilities for improvement of photovoltaic solar energy converters: Part I: considerations for earth's surface operation. ***Proc. IRE***, 1960; **48**(7): 1246–1263.

5 **Soga T.** Chapter 1 - fundamentals of solar cell. In: Soga T. (ed.), Nanostructured Materials for Solar Energy Conversion [Internet]. Amsterdam: Elsevier, 2006; pp. 3–43, Available from: https://www.sciencedirect.com/science/article/pii/B9780444528445500020.

6 **Saito T.** Spectral properties of semiconductor photodiodes. ***Adv. Photodiodes***, 2011; 21.

7 **Hovel H. J.** Semiconductors and semimetals. Volume 11. ***Solar cells***, 1975; Jan 1 [cited 2022 Mar 2]; Available from: https://www.osti.gov/biblio/7284142.

8 **Clerckx B., Popović Z., Murch R.** Future networks with wireless power transfer and energy harvesting [scanning the issue]. ***Proc. IEEE***, 2022; **110**(1): 3–7.

9 **Nguyen D. H.** Optical wireless power transfer for moving objects as a life-support technology. In: 2020 IEEE 2nd Global Conference on Life Sciences and Technologies (LifeTech). 2020; pp. 405–408.

10 **Bogushevskaya V., Zhalnin B., Zayats O., Maslyakov Y. N., Matsak I., Nikonov A. et al.** An experimental investigation of the feasibility of using silicone and gallium arsenide solar batteries on space vehicles for receiving energy of laser infrared emission. ***Therm. Eng.***, 2012; **59**(13): 975–980.

11 **Katsuta Y.**, **Miyamoto T.** Design and experimental characterization of optical wireless power transmission using GaAs solar cell and series-connected high-power vertical cavity surface emitting laser array. ***Jpn. J. Appl. Phys.***, 2018; **57**(8S2): 08PD01. 6.

12 **Matsuura M.**, **Nomoto H.**, **Mamiya H.**, **Higuchi T.**, **Masson D.**, **Fafard S.** Over 40-W electric power and optical data transmission using an optical fiber. ***IEEE Trans. Power Electron***, 2021; **36**(4): 4532–4539.

13 **Khvostikov V. P.**, **Kalyuzhnyy N. A.**, **Mintairov S. A.**, **Sorokina S. V.**, **Potapovich N. S.**, **Emelyanov V. M. et al.** Photovoltaic laser-power converter based on AlGaAs/GaAs heterostructures. ***Semiconductors***, 2016; **50**(9): 1220–1224.

14 **Duffie J. A.**, **Beckman W. A.**, **Blair N.** Solar Engineering of Thermal Processes, Photovoltaics and Wind. John Wiley & Sons, 2020.

15 **IEC 60904-3:2019** |IEC Webstore |water management, smart city, rural electrification, solar power, solar panel, photovoltaic, PV, LVDC [Internet]. [cited 2022 Mar 2]. Available from: https://webstore.iec.ch/publication/61084.

16 **Green M.A.** General solar cell curve factors including the effects of ideality factor, temperature and series resistance. ***Solid-State Electron***, 1977; **20**(3): 265–266.

17 **Lorenzo E.** Solar Electricity: Engineering of Photovoltaic Systems. Earthscan/James & James, 1994.

18 **Si photodiode S1227-1010BQ** |Hamamatsu Photonics [Internet]. [cited 2022 Mar 2]. Available from: https://www.hamamatsu.com/us/en/product/optical-sensors/photodiodes/si-photodiodes/S1227-1010BQ.html.

19 **Si photodiode S1337-1010BQ** |Hamamatsu Photonics [Internet]. [cited 2022 Mar 2]. Available from: https://www.hamamatsu.com/us/en/product/optical-sensors/photodiodes/si-photodiodes/S1337-1010BQ.html.

20 **Zalewski E.F.**, **Geist J.** Silicon photodiode absolute spectral response self-calibration. ***Appl. Opt.***, 1980; **19**(8): 1214–1216.

21 **Ohno Y.** Silicon photodiode self-calibration using white light for photometric standards: theoretical analysis. ***Appl. Opt.***, 1992; **31**(4): 466–470.